Temperature-Dependent Ratiometric Fluorescence from an Organic Aggregates System

Jie Huang,[†,‡] Aidong Peng,[†] Hongbing Fu,[†] Ying Ma,[†] Tianyou Zhai,[†,‡] and Jiannian Yao*[,†]

Beijing National Laboratory for Molecular Sciences (BNLMS), Key Laboratory of Photochemistry, Institute of Chemistry, Chinese Academy of Sciences, Beijing 100080, P. R. China, and Graduate University of the Chinese Academy of Sciences, Beijing 100039, P. R. China

Received: March 9, 2006; In Final Form: May 12, 2006

The aggregates of 2-(2′-hydroxyphenyl)benzoxazole (HBO), a typical molecule exhibiting excited-state intramolecular proton transfer (ESIPT), were prepared and the photophysical properties of the aqueous dispersion of aggregates were investigated. It is found that the aggregates and the solvated enols coexist in the aqueous dispersion system. Furthermore, the aggregates undergo ESIPT to give rise to keto for green emission, while the solvated enols give rise to blue emission. The temperature effects on the aqueous dispersion of the HBO aggregates system were also explored. It shows a fluorescent ratiometric change in a range of temperature from 15 to 60 °C. A mechanism of a temperature-dependent equilibrium between the aggregates and the solvated enols is proposed for the fluorescence change. The reversibility and robustness as well as the stability of the aqueous dispersion of aggregates show very good performances, which may be useful in the applications of molecular fluorescent temperature sensors or molecular thermometers.

Introduction

Molecular sensors have been extensively explored in the development of novel functional materials as well as the detection and measurement of various kinds of analytes. Especially, molecular fluorescent sensors[1] have received an increasingly enormous amount of attention because they have advantages in terms of high sensitivity, high selectivity, and the ease of detection in the fluorescence changes of the systems. The design principles and the operating mechanisms for these fluorescent sensors, such as photoinduced electron transfer (PET), electronic energy transfer (EET), charge transfer (CT), and so on, have been reviewed.[2−4] In addition, a number of these sensors are now commercially available.[5] However, the investigations of molecular fluorescent sensors to probe the environmental properties, such as temperature, despite being of fundamental and practical importance in a wide variety of systems, have received rare attention to date, and only a few reports on these probes[6−13] were found in the literature.

Molecules with an intramolecular hydrogen bond often undergo excited-state intramolecular proton transfer (ESIPT)[14] and have attracted considerable research interest in the development of novel materials such as UV-photostablizers, [15,16] laser dyes,[17,18] and fluorescent probes.[19−23] ESIPT is a photoinduced tautomerization that yields excited-state keto species from the enol species in the subpicosecond time scale even in rigid media and at temperatures down to 4 K. After the relaxation of the keto to the ground state, the enol is recovered spontaneously by a reverse proton transfer (PT) process. It has been, therefore, generally observed an abnormally large Stokes' shift without self-absorption, due to the emission of the keto as a result of the absorption from the enol. 2-(2′-Hydroxyphenyl)benzoxazole (HBO) (Scheme 1) is well-known as one of the typical molecules exhibiting ESIPT.[24−32] Its dual fluorescence is very attractive from the standpoint of fluorescent sensor design, especially in the ratiometric consideration. However, it is reported that the fluorescence properties of HBO are also rather complicated because of its solvent- and pH-dependent conformational isomerisms and photoinduced tautomerization.[33,34] The complexity of fluorescence of HBO has thus impeded the development of new fluorescent sensors based on its dual emission.

SCHEME 1: Chemical Structures of the Enol and Keto in the ESIPT Process of HBO

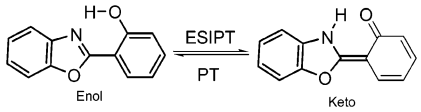

Herein, we report the temperature-dependent ratiometric change in emission of the HBO aggregates system. With a simple method,[35] an aqueous dispersion of HBO aggregates was easily and successfully obtained. The morphologies and structure of the as-prepared HBO aggregates were studied by scanning electron microscopy (SEM) and X-ray diffraction (XRD). The photophysical properties of the as-prepared aqueous dispersion of HBO aggregates were investigated by means of UV−visible absorption spectra as well as steady-state fluorescence spectra. It is found that the fluorescence of such a system displays a temperature-dependent change in the visible region of the spectrum ratiometrically, with very good performances in terms of reversibility, robustness, and stability, which may be potentially applicable in the design of temperature sensors.

Experimental Section

Materials. The compound investigated in our work, 2-(2′-hydroxyphenyl)benzoxazole (HBO), was purchased from ACORS, and was recrystallized from ethanol several times before use. HPLC grade dimethyl sulfoxide (DMSO), which was used as a good solvent, was purchased from ACORS and was used as received. Purified water with a resistivity of 18.2 MΩ·cm was

* Address correspondence to this author. Phone: +86-10-82616517. Fax: +86-10-82616517. E-mail: jnyao@iccas.ac.cn.
† Institute of Chemistry, Chinese Academy of Sciences.
‡ Graduate University of the Chinese Academy of Sciences.

10.1021/jp0614749 CCC: $33.50
Published on Web 06/30/2006

obtained through a Milli-Q water purification system (Millipore, Billerica, MA).

Methods. The HBO aggregates were prepared by a simple reprecipitation method.[35] In a typical preparation, 80 μL of a stock solution of HBO in DMSO (1.0×10^{-3} mol/L) was rapidly injected into 5 mL of water with vigorous stirring at an ambient temperature of 15 °C controlled by a thermocouple. HBO molecules began to aggregate at once as a result of the dramatic change of the solvent quality, thus, an aqueous dispersion of its aggregates was obtained.

The morphologies and sizes of the as-prepared HBO aggregates were examined on a scanning electron microscopy (SEM, Hitachi S-4300) at an accelerating voltage of 5 kV. For the preparation of SEM samples, the aqueous dispersion of HBO aggregates was filtered onto the surface of an alumina membrane with a pore size of 0.02 μm (Whatman International Ltd., U.K.). A layer of platinum was sputtered onto the surface to increase the conductivity of the samples, using a Ciko IB.3 Ion Coater at a current of 0.5 mA and a pressure of 3 mm Hg. The samples were then characterized on a D/max-2400 X-ray diffractometer with an X-ray source of Cu/K-R at 40 kV and 120 mA.

The UV−visible absorption spectra of the aqueous dispersion of HBO aggregates were measured on a Perkin-Elmer Lambda 35 spectrometer with a scanning speed of 480 nm/min and a slit width of 1 nm.

The steady-state excitation and emission fluorescence spectra of the aqueous dispersion of HBO aggregates were performed on a Hitachi F-4500 fluorescence spectrophotometer, using a right-angle configuration. Slits were set to provide widths of 5 nm for both the excitation and the emission monochromators in all cases.

For all the variable-temperature experiments, a thermostated cuvette holder connected to a constant-temperature water circulator was adapted to the spectrometers. The samples were equilibrated at each temperature for at least 10 min. Temperature was kept constant within ±1 K.

For the temperature cycles experiments, the spectra were obtained by alternatingly changing the temperature of the aqueous dispersion of HBO aggregates ranging from 15 to 60 °C, using the same devices as for the variable-temperature experiments.

The emission intensity ratios of keto to solvated enol (I_K/I_N) were determined by comparing fluorescence intensities at the wavelengths of 500 and 430 nm, respectively, and were uncorrected for differences in instrument response at the two wavelengths.

For all the measurements, the concentrations of the as-prepared aqueous dispersion of HBO aggregates were kept the same at 1.6×10^{-5} mol/L (the total HBO concentration).

Results and Discussion

The aqueous dispersion of HBO aggregates was successfully prepared in our investigation by utilizing a simple reprecipitation method.[35] Figure 1 shows some typical scanning electron microscopy images of the as-prepared HBO aggregates deposited onto the surface of an alumina membrane with a pore size of 0.02 μm from the aqueous dispersion. From the images, it can be seen that the aggregates are almost uniformly sheetlike with a diameter of ca. 1 μm. XRD measurements (see the Supporting Information) show that there exists one characteristic diffraction peak at 2θ of 7.78° (d = 11.35 Å), suggesting that the aggregates are preferred orientated to some extent.

The UV−visible absorption spectra of the aqueous dispersion of HBO aggregates with different aging time as well as its dilute solution in dimethyl sulfoxide (DMSO) are shown in Figure 2. In the case of DMSO solution, there exist three absorption peaks in the spectra. The absorption at ca. 321 nm is assigned to the anti-enol, the absorption at ca. 334 nm corresponds to the syn-enol, and the absorption at ca. 295 nm is attributed to the benzoxazole moiety. These results are consistent with those reported previously.[26,34b] At the same time, it shows that the absorption of HBO aggregates is obviously different from that of HBO in DMSO solution. Furthermore, the evolution of the absorption of HBO aggregates was investigated as a function of aging time, as depicted in Figure 2.

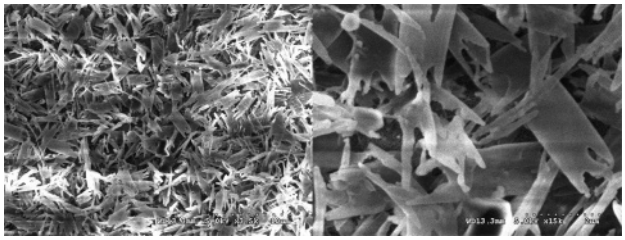

Figure 1. Typical scanning electron microscopy images of HBO aggregates: (left) low magnification and (right) high magnification. The samples were prepared by filtration of aqueous dispersion of HBO aggregates onto the surface of an alumina membrane with a pore size of 0.02 μm.

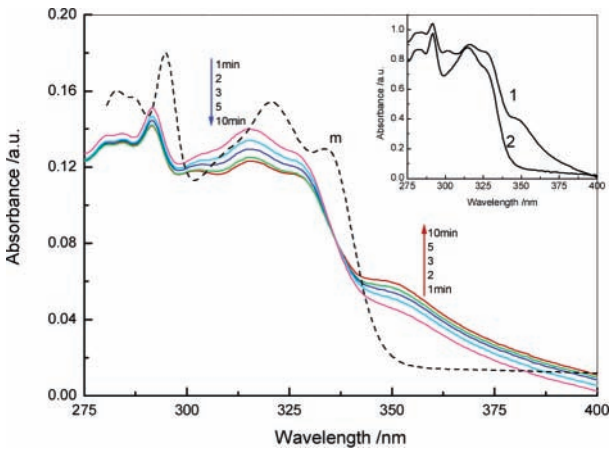

Figure 2. UV−visible absorption spectra of a DMSO solution of HBO (dashed line m) and the aqueous dispersion of its aggregates at different aging times at 15 °C (solid lines). Insert: UV−visible absorption spectra obtained before (1) and after (2) filtration of the aqueous dispersion of HBO aggregates (normalized for clarity).

As for the aqueous dispersion of HBO aggregates, the two $\pi-\pi^*$ absorption bands corresponding to the enols were blue-shifted as compared with that of HBO in DMSO solution. In addition, there appears a new broad and structureless absorption band centered at ca. 350 nm. After filtration of the aqueous dispersion, the new absorption band disappears (insert in Figure 2). Thus, we can assign this new broad band to the absorption of the aggregates. At the same time, the new absorption band increases gradually while the enol absorption bands decrease gradually with increasing aging time, indicating the process of aggregation. An apparent isobestic point at 336 nm is also observed, which can be the evidence for the coexistence of the dissolved enols and aggregates. It can be seen that from about 10 min onward, changes of the spectra are minimal, suggesting that the aggregation process reaches a plateau.

The fluorescence spectra of the aqueous dispersion of HBO aggregates with different aging time in comparison with its dilute solution in dimethyl sulfoxide (DMSO) are shown in Figure 3. In DMSO solution, the fluorescence spectrum shows a strong emission band centered at ca. 367 nm, which can be assigned

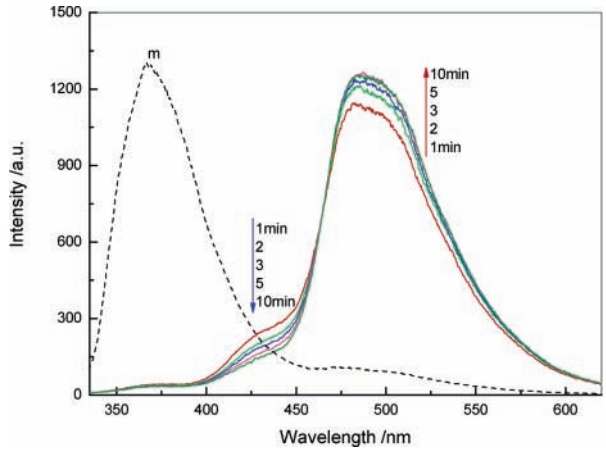

Figure 3. Fluorescence emission spectra of a DMSO solution of HBO (dashed line m) and the aqueous dispersion of its aggregates at different aging times at 15 °C (solid lines). The excitation wavelength is at the isobestic point, 336 nm.

to the enol emission, together with a weak but detectable broad band in the region of 455−550 nm, corresponding to the keto emission. These results are in good agreement with those in the literature.[26,34b] However, it is found that in the case of aggregates, the emission bands are composed of an intense broad band centered at ca. 500 nm, along with a weak shoulder at ca. 430 nm.

To figure out the origin of the fluorescent species, we measured the fluorescence emission spectra at various excitation wavelengths as well as excitation spectra at various emission wavelengths, as shown in Figure 4. The emission spectra obtained upon excitation at 320 and 350 nm are obviously different, whereas there is no shoulder peak at ca. 430 nm in the latter case, suggesting that the emissions come from different species. As can be clearly seen in Figure 4, the excitation spectra show distinctness as well. There is an additional shoulder peak at ca. 350 nm in the spectrum when monitored at 500 nm, the position of which is consistent with that of the new absorption peak shown in Figure 2. These results altogether evidently show that the contribution to the emission stems from two totally different species experiencing distinct excitation processes. The above interpretations are also supported by an apparent isoemissive point at ca. 455 nm as depicted in Figure 3, indicating the presence of two species in the excited state as well.

For the broad low-energy band, we can assign it to the keto emission due to the characteristic abnormally large Stokes' shift. It should be noted that this emission is almost identical with that of its solid powder upon excitation at 350 nm located at the absorption region of the aggregates (see the Supporting Information). Thus, it is unambiguous that the aggregates undergo ESIPT to give birth to the keto emission.

It has been reported that emission of HBO from both enol and keto is observed with intensities that strongly depend on solvents.[34] It is also well-known that the water molecule has the strong ability to form hydrogen bonds with other molecules. The intermolecular hydrogen bonds between the water molecules and the dissolved HBO molecules are thus expected in the aqueous dispersion of HBO aggregates, which inhibited ESIPT and the emission of keto, despite the low solubility of HBO in water. To provide direct support for this, we present further experimental evidence.

The fluorescence properties of HBO in water were examined (see the Supporting Information) and the results showed that there was only one broad symmetrical peak centered at ca. 440 nm without a characteristic emission of the keto at a longer wavelength, indicating the predominant formation of the intermolecular hydrogen bond species that could not undergo ESIPT.[36] It was also found that the shoulder emission peak position in the aqueous dispersion of aggregates was very close to that in water when excited at 320 nm, and that the excitation spectra were identical with each other when monitored at 430 nm. Thus, it is reasonable that the solvated enol species give rise to the shoulder emission at ca. 430 nm in the case of aggregates in that the intermolecular hydrogen bond between the water molecule and the dissolved HBO molecule in the aqueous dispersion of HBO aggregates inhibited ESIPT and the emission of keto.

As can be seen in Figure 3, the fluorescence intensity of the keto in the case of aggregates is almost 14-fold that in DMSO solution. ESIPT in our case is fairly favored probably due to the increased planarity and rigidity exerted by the aggregation. Furthermore, the excited-state intermolecular proton transfer is also possible as a result of a large quantity of adjacent close-packed molecules in the aggregates. The enhanced keto emission in HBO aggregates is, therefore, anticipated. Meanwhile, the evolution of fluorescence emission of HBO aggregates was also studied as a function of aging time, as displayed in Figure 3. The fluorescence intensity of keto increases gradually while that of solvated enols decreases gradually with increasing aging time, with an isoemissive point at ca. 455 nm, suggesting the existence of the aggregates and the solvated enols in the excited state. However, it should be noted that there are no palpable changes 10 min later, indicating that a steady state of such a system is achieved.

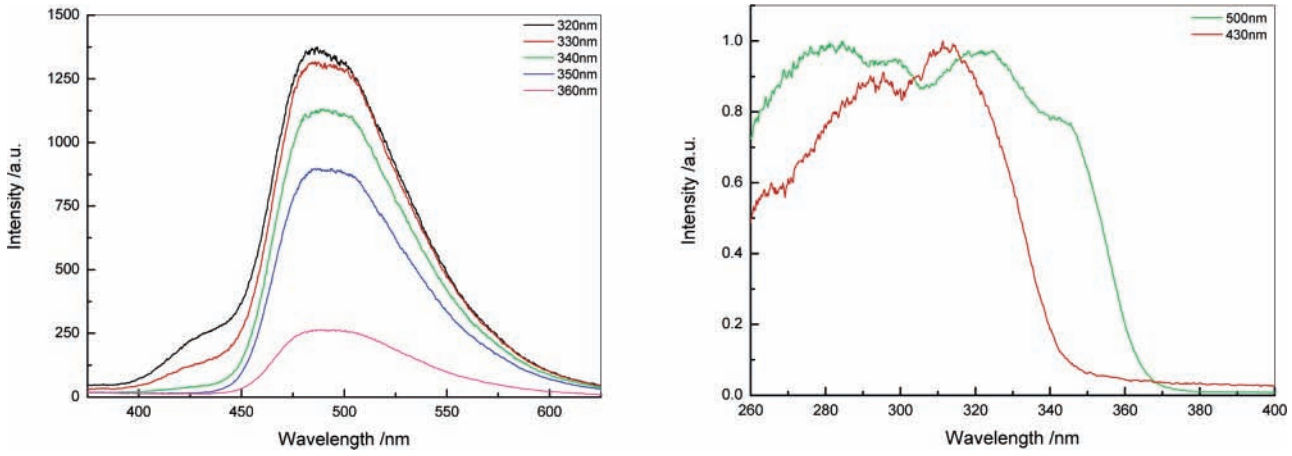

Figure 4. Fluorescence emission (left) and excitation (right) spectra of the aqueous dispersion of HBO aggregares at 15 °C.

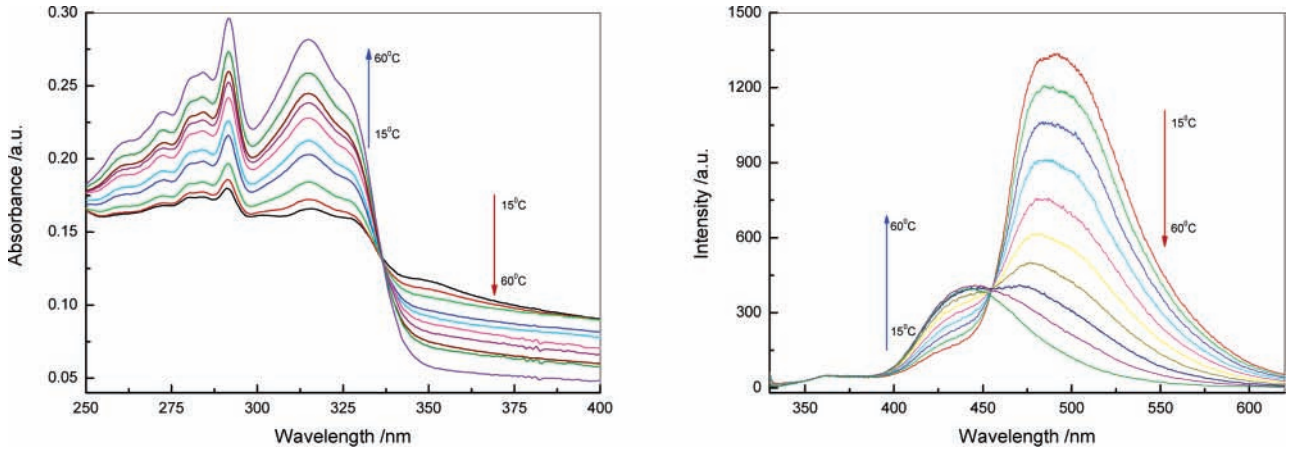

Figure 5. Temperature-dependent UV−visible absorption (left) and fluorescence emission (right) spectra of the aqueous dispersion of HBO aggregates at a temperature interval of 5 °C. The excitation wavelength is at the isobestic point, 336 nm.

SCHEME 2: Schematic Illustration of the Proposed Temperature-Dependent Equilibrium between the Solvated Enol and the Aggregates

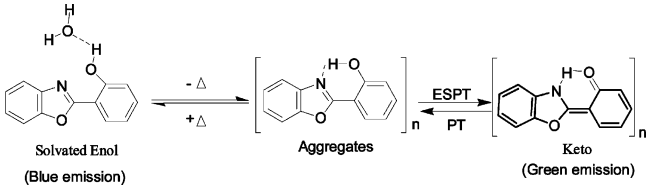

The effects of temperature on the absorption and emission of the aqueous dispersion of HBO aggregates are illustrated in Figure 5. It displays that the emission intensity of keto decreases gradually while that of solvated enol increases gradually with rising temperature under control. The changes are reversible. To the best of our knowledge, this is the first report on the temperature-dependent ratiometric change in emission of an organic aggregates system. It is reported that temperature has no appreciable effect on the rate of the ESIPT process of HBO in various kinds of organic solvents, which suggests that there exists no obvious potential barrier for the adiabatic ESIPT process.[34a] Therefore, in our case, the changes of fluorescence may not be interpreted as a result of a temperature-dependent ESIPT process. Principally, temperature has an intrinsic effect on the fluorescence quantum yield of the chromophore.[37] However, temperature can also exert other extrinsic effects on fluorescence, such as shifting equilibria between some specific processes,[10,13] states,[7,8,11,12] and so on. As has been discussed before, there coexist two species, namely, the solvated enols and the aggregates in our case. On the basis of the above results, we ascribe the temperature-dependent fluorescence to the shift of the equilibrium between the two species. A simple schematic illustration of this is presented in Scheme 2. The equilibrium shifts gradually toward the left to give rise to blue emission by increasing temperature while shifts toward the right to give rise to green emission by cooling the sample. This is evidently supported by the existence of an apparent isoemissive point at ca. 455 nm as shown in Figure 5. At the same time, when the aqueous dispersion of HBO aggregates was heated slowly, the absorption of the aggregates decreased slowly while that of the solvated enols increased slowly. The changes are reversible as well. The proposed temperature-dependent equilibrium mechanism is thus once again confirmed by an obvious isobestic point at 336 nm in the temperature-dependent UV−visible spectra, as displayed in Figure 5. The relationship between the emission intensity ratio of keto to solvated enol (I_K/I_N) and temperature

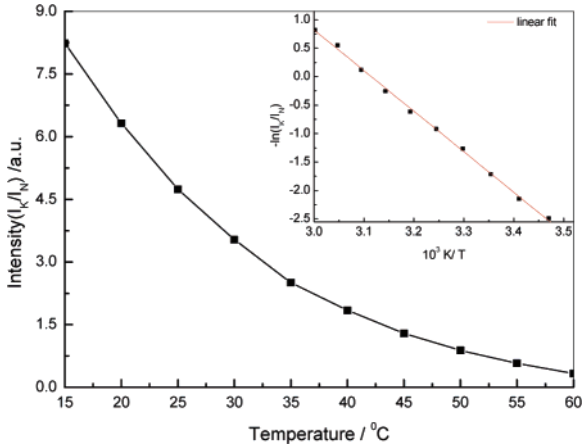

Figure 6. Plot of the emission intensity ratio of keto to solvated enol, I_K/I_N, against temperature in the aqueous dispersion of HBO aggregates. The insert is a plot and its linear fit (solid line) of the negative natural logarithm of the emission intensity ratio of keto to solvated enol, I_K/I_N, as a function of reciprocal temperature.

is shown in Figure 6. The emission intensity ratio, I_K/I_N, decreases with the increase in temperature, which may allow the sensing of temperature ratiometrically. Moreover, the enthalpy of the aggregates to the solvated enol equilibrium can be determined from the slope of the curve (insert in Figure 6), in which a relationship between the negative logarithm of I_K/I_N and the reciprocal of temperature is present, and is thus calculated to be -59.2 ± 0.8 kJ/mol after a reasonably good linear fit. It is worthy to point out that a marked feature of the interconversion with temperature is the presence of blue emission under hot conditions and green emission as the sample is cooled, upon irradiation with a hand-held UV light. A picture is shown in Figure 7 to give a direct visual demonstration.

To investigate the reversibility and robustness of the ratiometric changes, we carried out the temperature cycles experiments, as shown in Figure 8. The results reveal that the reversibility is still maintained after 10 repeated cycles between temperatures from 15 to 60 °C, showing a very good robustness. In addition, we have observed the same reversible ratiometric changes with no remarkable variation in intensities even one month later, indicating its excellent stability. The good reversibility and robustness as well as the stability of such a system may be applicable in the temperature sensing.

Conclusions

In summary, we have successfully prepared the HBO aggregates with the reprecipitation method. Two fluorescent

Figure 7. The visual pictures of the aqueous dispersion of HBO aggregates at low (15 °C) and high (60 °C) temperatures upon irradiation of a hand-held UV light.

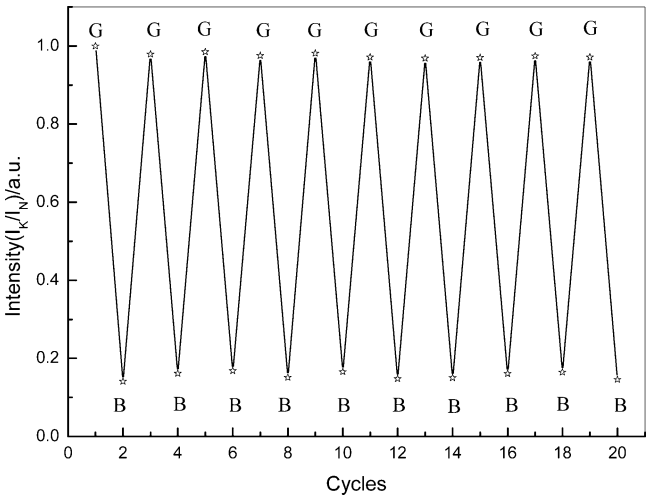

Figure 8. Demonstration of the reversible and robust fluorescence intensity ratio of I_K/I_N by alternating temperatures at 15 (G) and 60 °C (B) in the aqueous dispersion of HBO aggregates.

species are identified in the aqueous dispersion of HBO aggregates by means of UV−visible absorption and steady-state fluorescence measurements. The blue emission is attributed to the solvated enols, while the green emission is ascribed to the aggregates undergoing ESIPT to give rise to keto. It exhibits a fluorescent ratiometric change in an amiable range of temperature from 15 to 60 °C in the aqueous dispersion of the aggregates. The changes have been interpreted as a result of the shift of the temperature-dependent equilibrium between the solvated enols and the aggregates. The reversibility and robustness as well as the stability of the system show a very good performance. The investigations here present a successful demonstration, which may be useful in the strategy for a fluorescent temperature sensor design and the applications of molecular fluorescent temperature sensors or molecular thermometers in the future.

Acknowledgment. This work was supported by the National Natural Science Foundation of China (Nos. 50221201, 90301010, 20373077, 20471062, and 50573084) and the Chinese Academy of Sciences.

Supporting Information Available: XRD patterns of HBO powder and aggregastes, the fluorescence emission spectrum of HBO powder, and the fluorescence spectra of HBO in water. This material is available free of charge via the Internet at http://pubs.acs.org.

References and Notes

(1) (a) de Silva, A. P.; Tecilla, P. *J. Mater. Chem.* **2005**, *15*, 2637 and references therein. (b) de Silva, A. P.; McClenaghan, N. D. *Chem. Eur. J.* **2004**, *10*, 574. (c) Demchenko, A. P. *Trends Biotechnol.* **2005**, *23*, 456 and references therein. (d) Prodi, L. *New J. Chem.* **2005**, *29*, 20. (e) Wiskur, S. L.; Ait-Haddou, H.; Lavigne, J. J.; Anslyn, E. V. *Acc. Chem. Res.* **2001**, *34*, 963. (f) Czarnik, A. W. *Fluorescent Chemosensors for Ion and Molecule Recognition*; American Chemical Society: Washington, DC, 1993.

(2) (a) Callan, J. F.; de Silva, A. P.; Magri, D. C. *Tetrahedron* **2005**, *61*, 8551. (b) de Silva, A. P.; Gunaratne, H. Q. N.; Gunnlaugsson, T.; Huxley, A. J. M.; McCoy, C. P.; Rademacher, J. T.; Rice, T. E. *Chem. Rev.* **1997**, *97*, 1515. (c) Bissell, R. A.; de Silva, A. P.; Gunaratne, H. Q. N.; Lynch, P. L. M.; Maguire, G. E. M.; McCoy, C. P.; Sandanayake, K. R. A. S. *Top.Curr. Chem.* **1993**, *168*, 223. (d) Bissell, R. A.; de Silva, A. P.; Gunaratne, H. Q. N.; Lynch, P. L. M.; Maguire, G. E. M.; Sandanayake, K. R. A. S. *Chem. Soc. Rev.* **1992**, 187.

(3) Valeur, B.; Leray. I. *Coord. Chem. Rev.* **2000**, *205*, 3.

(4) Wason, W. T. *Fluorescent and Luminescent Probes for Biological Activity*; Academic Press: San Diego, CA, 1999.

(5) Haugland, R. P. *Handbook of Fluorescent Probes and Research Products*; Molecular Probes: Eugene, OR, 2002.

(6) (a) Uchiyama, S.; Matsumura. Y.; de Silva, A. P.; Iwai, K. *Anal. Chem.* **2004**, *76*, 1793. (b) Uchiyama, S.; Matsumura. Y.; de Silva, A. P.; Iwai, K. *Anal. Chem.* **2003**, *75*, 5926.

(7) Baker, G. A.; Baker, N. S.; Mccleskey, T. M. *Chem. Commun.* **2003**, 2932.

(8) Chandrasekharan, N.; Kelly, L. A. *J. Am. Chem. Soc.* **2001**, *123*, 9898.

(9) Brewster, R. E.; Kidd, M. J.; Schuh, M. D. *Chem. Commun.* **2001**, 1134.

(10) Seeboth, A.; Kriwanek, J.; Vetter, R. *Adv. Mater.* **2000**, *12*, 1424.

(11) Engeser, M.; Fabbrizzi, L.; Liccheui, M.; Sacchi, D. *Chem. Commun.* **1999**, 1191

(12) Figueroa, I. D.; Baraka, M. E.; Quinones, E.; Rosario, O. *Anal. Chem.* **1998**, *70*, 3974.

(13) Lou, J.; Hatton, T. A.; Laibinis, P. E. *Anal. Chem.* **1997**, *69*, 1262.

(14) (a) Arnaut, L. G.; Formosinho, S. J. *J. Photochem. Photobiol. A: Chem.* **1993**, *75*, 1. (b) Formosinho, S. J.; Arnaut, L. G. *J. Photochem. Photobiol. A: Chem.* **1993**, *75*, 21.

(15) Luiz, M.; Biasttti, A.; Soltermann, A. T.; Garcia, N. A. *Polym. Degrad. Stab.* **1999**, *63*, 447.

(16) O'Connor, D. B.; Scott, G. W.; Goulter, D. R.; Yavroulan, A. *J. Phys. Chem.* **1991**, *95*, 10252.

(17) Tarkka, R. M.; Zhang, X.; Jenekhe, S. A. *J. Am. Chem. Soc.* **1996**, *118*, 9438.

(18) Chou, P.-T.; Martinez, M. L.; Clements, J. H. *J. Phys. Chem.* **1993**, *97*, 2618.

(19) Henary, M. M.; Wu, Y.-G.; Fahrni, C. J. *Chem. Eur. J.* **2004**, *10*, 3015.

(20) Ohshima, A.; Momotake, A.; Arai, T. *Tetrahedron Lett.* **2004**, *45*, 9377.

(21) Klymchenko, A. S.; Demchenko, A. P. *J. Am. Chem. Soc.* **2002**, *124*, 12372.

(22) Tanaka, K.; Kumagai, T.; Aoki, H.; Deguchi, M.; Iwata, S. *J. Org. Chem.* **2001**, *66*, 7328.

(23) Sytnik, A.; Delvalle, J. C. *J. Phys. Chem.* **1995**, *99*, 13028.

(24) Williams, D. L.; Heller, A. *J. Phys. Chem.* **1970**, *74*, 4473.

(25) Nakagaki, R.; Kobayashi, T.; Nagakura, S. *Bull. Chem. Soc. Jpn.* **1978**, *51*, 1671.

(26) Woolfe, G. J.; Melzig, M.; Schneider, S.; Dörr, F. *Chem. Phys.* **1983**, *77*, 213.

(27) Itoh, M.; Fujiwara, Y. *J. Am. Chem. Soc.* **1985**, *107*, 1561.

(28) Tero-Kubota, S.; Akiyama, K.; Shoji, F.; Ikegami, Y. *J. Chem. Soc., Chem. Commun.* **1992**, 641.

(29) Roberts, E. L.; Dey, J.; Warner, I. M. *J. Phys. Chem. A* **1997**, *101*, 5296.

(30) Abou-Zied, O. K.; Jimenezm, R.; Romesberg, F. E. *J. Am. Chem. Soc.* **2001**, *123*, 4613.

(31) Taki, M.; Wolfood, J. L.; O'Halloran, T. V. *J. Am. Chem. Soc.* **2004**, *126*, 712.

(32) Ogoshi, T.; Miyake, J.; Chujo, Y. *Macromolecules* **2005**, *38*, 4425.

(33) (a) Krishnamurthy, M.; Dogra, S. K. *J. Photochem.* **1986**, 32, 235. (b) Elsassler, T.; Schmetzer, B. *Chem. Phys. Lett.* **1987**, *140*, 293.

(34) (a) Das, K.; Sarkar, N.; Ghosh, A. K.; Majumdae, D.; Nath, D. N.; Bhattacharyya, K. *J. Phys. Chem.* **1994**, *98*, 9126. (b) Abou-Zied, O. K.; Jimenezm, R.; Thompson, E. H. Z.; Millar, D. P.; Romseberg, F. E. *J. Phys. Chem. A* **2002**, 106, 3665.

(35) (a) Kasai, H.; Nalwa, H. S.; Oikawa, H.; Okada, S.; Matsuda, H.; Minami, N.; Kakuta, A.; Ono, K.; Mukoh, A.; Nakanishi, H. *Jpn. J. Appl. Phys., Part 2* **1992**, *31*, L1132. (b) Fu, H.-B.; Yao, J.-N. *J. Am. Chem. Soc.* **2001**, *123*, 1434.

(36) (a) Rois, M. A.; Rois, M. C. *J. Phys. Chem.* **1995**, *99*, 12456. (b) Seo, J.; Kim, S.; Park, S. Y. *J. Am. Chem. Soc.* **2004**, *126*, 11154.

(37) Valeur, B. *Molecular Fluorescence*; Wiley-VCH: Weinheim, Germany, 2002.